Proceedings of the Sixth International Conference on
Railway Technology: Research, Development and Maintenance
Edited by: J. Pombo
Civil-Comp Conferences, Volume 7, Paper 3.10
Civil-Comp Press, Edinburgh, United Kingdom, 2024
ISSN: 2753-3239, doi: 10.4203/ccc.7.3.10

Aerodynamic Characteristics of High-Speed Train Entering and Leaving Tunnel Under Gorge Wind

D. Guo[1], J. Chen[1], D. Chen[2] and G. Yang[1]

[1]Key Laboratory for Mechanics in Fluid Solid Coupling Systems, Institute of Mechanics, Chinese Academy of Sciences, Beijing, China
[2]National Engineering Research Center for High-speed EMU, CRRC Qingdao Sifang Co., Ltd., China

Abstract

The terrain of mountainous valleys is complex, and the distribution of wind speed along the railway is affected by the terrain of the valleys, resulting in uneven distribution of wind speed inside the valleys. Under the influence of the wind field in the gorge, the aerodynamic loads of the train when crossing bridges and tunnels change violently, causing a sudden increase in wheel-rail force, and reducing the safety of the train. In this paper CRH380A three-marshalling high-speed EMU is taken as the research object. the gorge wind field model is applied to the train running across the bridge and tunnel, and the effects of the gorge wind field model and the constant wind field model on the train's aerodynamic characteristics are compared. In the process of the train running across the bridge and tunnel, the difference in the aerodynamic load of each section under different wind fields is mainly reflected in the process of the train entering and leaving the wind field, and the transition section across the bridge and tunnel. The change rate and fluctuation amplitude of each aerodynamic load under a constant wind field are greater than those under gorge wind conditions.

Keywords: wind field model, high-speed train, gorge wind, entering and leaving tunnel, aerodynamic load, numerical simulation.

1 Introduction

When the train runs across the bridge and tunnel between mountain gorges, because each section of the car body suddenly enters or leaves the wind field in turn, it not

only produces complex flow around the train, but also makes the load on each section of the car body different and has strong abrupt change. It is easy to occur the operation instability caused by the complex aerodynamic effect caused by the sudden change of flow field, and even lead to major safety accidents such as train derailment and capsizing [1-5]. The existing research shows that the aerodynamic load on the train has an important influence on the safety indexes such as critical speed, derailment coefficient, wheel load reduction rate and so on [6]. For the environment like mountain gorge, the uneven distribution of wind field and the acceleration effect of wind speed cause the train to face more complex crosswind environment in the process of running across bridges and tunnels. By comparing the aerodynamic characteristics of the high-speed train in the wind field of the constant wind and rain canyon, this paper studies the aerodynamic characteristics and flow mechanism of the train running across the bridge and tunnel. The research results can provide guidance for train dynamics calculation and the establishment of mountain canyon train speed safety region.

2 Train model and calculation method

2.1 Train model and calculation domain

The real train model CRH380A was adopted, as shown in Figure 1.

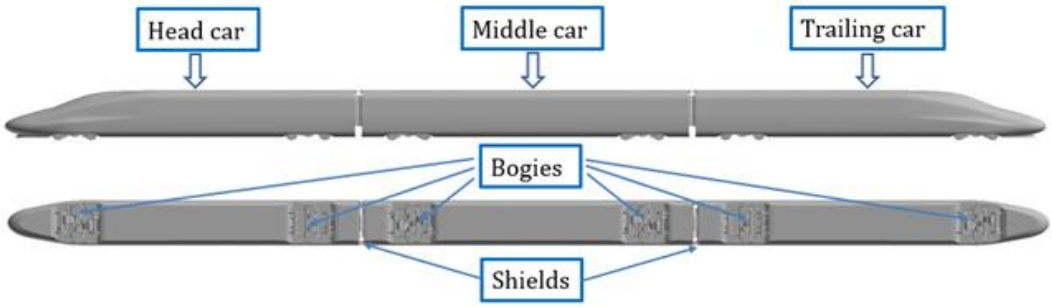

Figure 1 Calculation model CRH380A

In order to simulate the whole process of the train leaving the tunnel, passing through the bridge and entering the tunnel in the gorge, the calculation domain is divided into five parts. Domain 1 is the starting operation area of the train, domain 2 is the tunnel area before the train enters the canyon wind field, domain 3 is the bridge area where there is a canyon wind field in the middle of the canyon mountain, and Domain 4 is the tunnel area after leaving the canyon wind field. The calculation domain 5 is the outer area of the tunnel after driving out of the wind field. The distance from the train floor to the top of train H (3.55m) is taken as the characteristic length, and the dimensions of each area are shown in Figure 2. The tunnel section is shown in Figure 3.

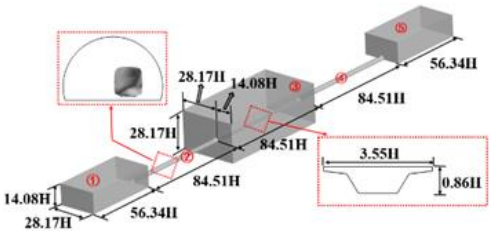

Figure 2 Schematic diagram of the calculation domain

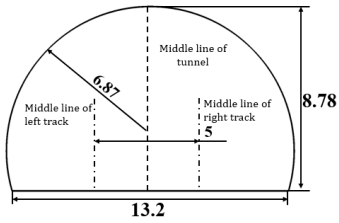

Figure 3 Cross-section dimensions of double track tunnel (unit: m)

Boundary conditions: except for the non-slip wall surface of the ground, the other five surfaces of domains 1 and 5 are pressure outlet boundaries, the tunnels of domains 2 and 4 are also set to non-slip wall, and domain 3 is the gorge wind flow zone. the boundary conditions of the inlet surface are set as the velocity inlet, and the upper and lower boundaries and outlet surfaces of the bridge deck are set as the pressure outlet.

2.2 Calculation method and grid setting

In the process of a high-speed train running across the bridge and tunnel, on the one hand, it is alternately affected by compression wave and expansion wave, on the other hand, it is also affected by the canyon wind. The wake and leeward side of the train also contain many kinds of eddies of different scales, and the flow field is very complex. To accurately simulate the aerodynamic force of each section, the RANS calculation method based on the SST k-ω turbulence model is used to calculate, and the standard wall function is used to simulate the wall turbulence. By setting the height of the grid in the first layer of the wall, the y + value falls well within the best applicable range (30~150). The governing equation is the unsteady N~S equation. When unsteady calculation, the time step is 2×10^{-3}s, the inner iterative step is 5, and the internal iterative residual is reduced by at least one order of magnitude.

To simulate the relative motion between the train, the tunnel, and the bridge, the overlapping grid technique is used for calculation. The component grid in this paper is the overset grid containing the train, and the background grid is the whole computing domain grid. The size of the car body overset grid is 0.25m, the total amount of the car body overset grid is about 12 million, and the maximum size of the calculation domain grid is about 2m. Two encrypted areas are set near the train running route. The grid size of the inner encryption area is 0.25m, which meets the requirement of overlapping at least 4-5 layers between the component grid and the background grid. The grid size of the outer encryption area is 0.5m, and the total amount of the background grid is about 21 million. The diagram of the grid model is shown in Figure 4.

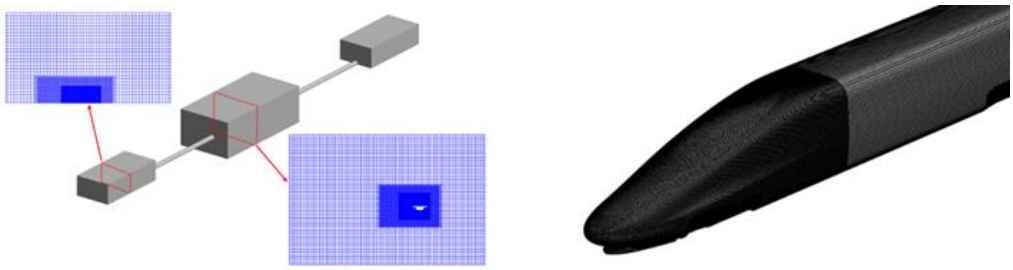

(a) Background grid (b) Car body grid

Figure 4 Schematic diagram of local grid

3 Aerodynamic load characteristics of trains under different wind fields

In this paper, the aerodynamic load characteristics and flow field characteristics of constant wind field and canyon wind field are compared by taking the working conditions of speed 350km/h and wind speed 15m/s as examples.

3.1 Different wind field description

Different wind field models have an important influence on the aerodynamic load of the train. The constant wind field model and the canyon wind field model in reference [36] are selected.

The constant wind field model does not change with the change of spatial coordinates, that is, the train enters the constant wind field immediately after leaving the tunnel at one end of the canyon, as shown in figure 5.

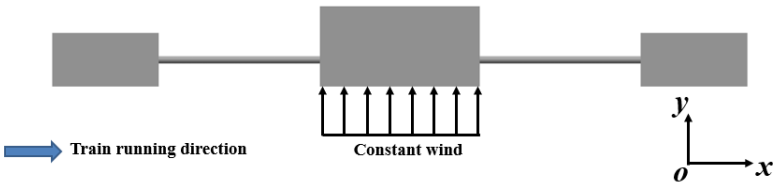

Figure 5 Schematic diagram of uniform wind field

The schematic diagram of the canyon wind field is shown in Figure 6.

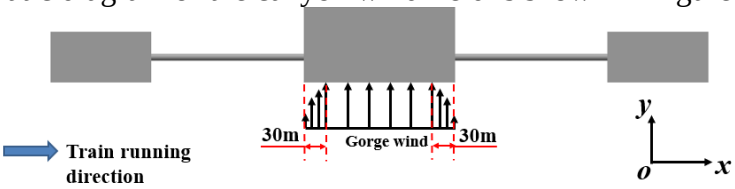

Figure 6 Schematic diagram of the gorge wind field

The wind field model is applied to the calculation domain by changing the boundary conditions. the constant wind field is directly given the wind speed as 15m/s, and the canyon wind field is applied by a given piecewise function at the velocity entrance boundary. The canyon wind field is shown in Formula 8 [7].

$$\begin{cases} U = 15 \times \left(\dfrac{x - 380}{30} \right)^{0.3}, \ 380 \le x \le 350 \\ U = 15, \ 350 < x \le 650 \\ U = 15 \times \left(\dfrac{680 - x}{30} \right)^{0.3}, \ 650 < x \le 680 \end{cases} \tag{1}$$

3.2 Comparison of aerodynamic load characteristics of trains entering wind field

The main difference between the canyon wind field and the constant wind field lies in the wind speed distribution near the mountain wall, that is, in the 30m area of the transition section between the mountain tunnel and the bridge, the difference of the aerodynamic load of the train under different wind fields is mainly reflected in this area.

Figure 7 shows the comparison of the aerodynamic time history curves of the first train entering the wind field under different wind fields. The time when the head car arrives near the entrance of the bridge tunnel (t = 3.8s) is taken as the initial time, and the time at which the nose cone of the tail car passes through the entrance of the bridge girder is taken as the end time (t = 5s). For the resistance of the first car, as the first car drives out of the tunnel and enters the wind field, due to the sudden opening of the flow space in front of the first car and the sudden decrease of resistance, there is no significant difference in the resistance curves between the two wind field models. For lateral force and lift, it can be seen from Fig. 7 (b) and (c) that the lateral force and lift increase obviously with the first car driving out of the tunnel under the two kinds of wind fields, the increase of lateral force is as high as 30kN and the increase of lift is as high as 20kN, but without crosswind, the lateral force and lift do not increase significantly. When the head car arrives at the exit of the tunnel, because the crosswind speed of the constant wind field is fixed, the lateral force and lift of the head car suddenly increase, while the wind speed of the canyon wind field increases gradually due to the existence of the boundary layer, and the increasing rate of lateral force and lift is lower than that of the constant wind field. there is no significant difference in the amplitudes of lateral force and lift under the two wind field models. It can be seen from Figure 7 (d),(e),(f) that after the head car enters the wind field, the absolute value of the overturning moment under the action of the two wind fields increases obviously, and the growth rate of the overturning moment under the constant wind field is higher than that in the canyon wind field, the pitching torque fluctuates obviously in the process of entering the wind field under the constant wind field, while there is no obvious fluctuation in the gorge wind field. the growth rate and amplitude of the yaw torque of the head car under the constant wind field are larger than that of the canyon wind field.

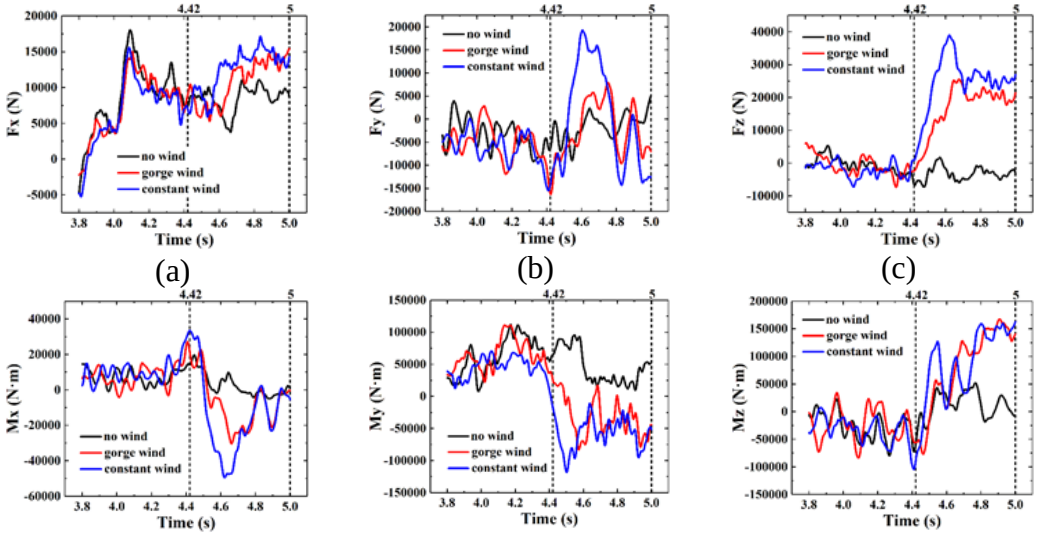

Figure 7 Aerodynamic load time history curves of the leading car (t=3.8s ~ 5s)

Figure 8 shows the comparison of the aerodynamic time history curves of the rear car entering the wind field under different wind fields. the windshield of the tail car of taper 4.42s reaches the entrance of the tunnel, and the nose cone of the tail of taper 5s reaches 30m outside the entrance of the tunnel. From the resistance curve, it can be seen that the overall amplitude of the tail car resistance under the action of the constant wind field is greater than that under the canyon wind field, and the increase of the tail car resistance is faster than that under the canyon wind field. There is a large abrupt change in the lateral force of the tail car in the constant wind field, and the lateral force of the tail car suddenly increases and then decreases, which is due to the large crosswind at the exit of the tunnel. As the tail car enters the wind field, the side wind contact area of the car body is larger, and the lateral force increases gradually. After the tail car completely enters the wind field, the lateral force decreases gradually because of the large upwind velocity of the airflow in the streamlined area of the tail and the existence of a low-pressure region. The sudden increase of lift, overturning moment, pitching moment, and yaw moment in the process of driving into the wind field under the constant wind field is larger than that in the canyon wind field.

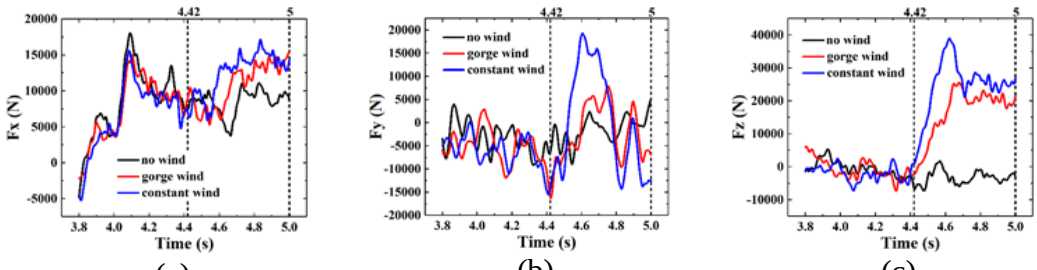

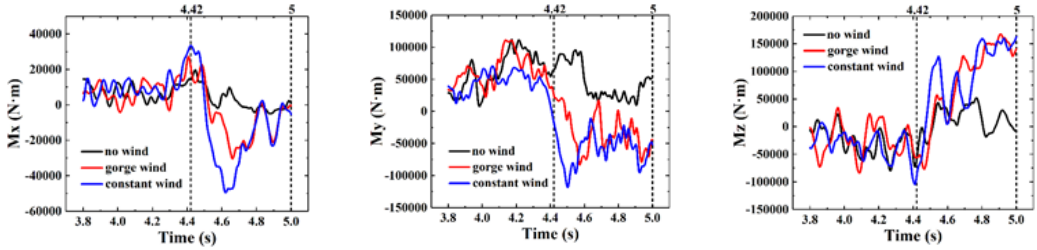

(d) (e) (f)

Figure 8 Aerodynamic load time history curves of trailing car (t=3.8s ~ 5s)

3.3 Comparison of aerodynamic load characteristics of trains leaving the wind field

Figure 9 shows the comparison of the aerodynamic time history curves of the first train leaving the wind field under different wind fields. As shown in Figure 9a, in the process of driving out of the wind field, the difference in head car resistance under the action of different wind fields is relatively small. It can be seen from Figure 9b that the lateral force under the two wind fields is different. The lateral force under the canyon wind field begins to decrease earlier than that under the constant wind field, and the lowest peak value of the lateral force under the constant wind field is lower than that under the canyon wind field. The main difference in the lift of the first car is that the decline rate of lift in the canyon wind field is lower than that in the constant wind field, and there is no significant difference in amplitude. As can be seen in Figure 14d, the difference in the overturning moment of the head car is mainly reflected in the decreasing rate when driving out of the wind field, and the decreasing rate of the overturning moment in the constant wind field is greater than that in the canyon wind field. The difference between the pitching torque and yaw torque of the head car is mainly reflected in the fluctuation in the process of driving out of the wind field, and the fluctuation of pitching torque in the constant wind field is larger than that in the canyon wind field.

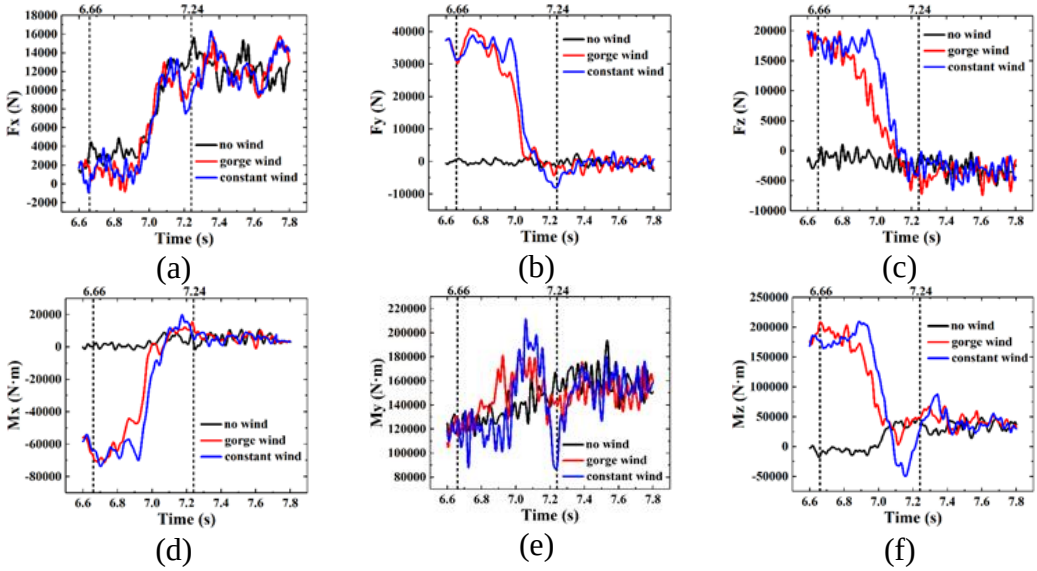

(a) (b) (c)

(d) (e) (f)

Figure 9 Aerodynamic load time history curves of leading car (t=6.6s ~ 7.8s)

Figure 10 shows the comparison of the aerodynamic time history curves of the rear car leaving the wind field under different wind fields. Among them, the nose cone of the tail car of taper 7.2s reaches the position 30m away from the exit tunnel of the bridge, and the windshield of the tail car of taper 7.78s reaches the exit tunnel of the bridge. As can be seen from the picture, in the process of driving out of the wind field, the aerodynamic force difference of the rear car under different wind fields is also relatively small compared with the front car. The peak value of resistance and lateral force in a constant wind field is larger than that in a canyon wind field. There is no significant difference in the performance of the overturning moment under the two kinds of wind fields, and the fluctuation of the overturning moment under the condition of no wind is larger than that under the condition of no wind. The other aerodynamic loads show that the decreasing rate of the constant wind field is higher than that of the canyon wind field.

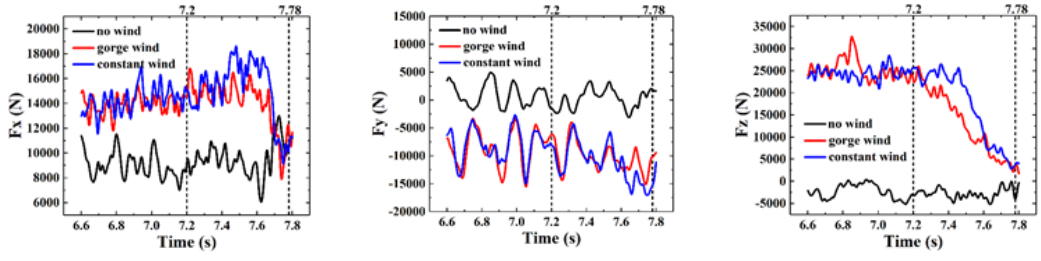

(a) (b) (d)

(e) (f) (f)

Figure 10 Aerodynamic load time history curves of trailing car (t=6.6s ~ 7.8s)

4 Conclusions and Contributions

The wind field model has an obvious influence on the aerodynamic characteristics of the high-speed train running across the bridge and tunnel, and the real and reasonable wind field model is helpful in accurately calculating the dynamic characteristics and safety of the train operation. The effects of the canyon wind field model and constant wind field model on train aerodynamic characteristics are compared, and the following conclusions are obtained.

(1)In the process of the train running across the bridge and tunnel, the difference of the aerodynamic load between the constant wind field and the canyon wind field is mainly reflected in the process of the train entering the wind field and leaving the wind field. the area in different wind fields mainly lies in the change rate and fluctuation amplitude of aerodynamic load, and the change rate and fluctuation

amplitude of each aerodynamic load in a constant wind field are larger than those in canyon wind conditions.

(2)In the process of entering the wind field, the instantaneous difference of the aerodynamic load under the two wind fields at different times is also very obvious, and the maximum instantaneous difference of the overturning moment of the head car under the two wind fields is as high as 68.4% of the average value under the canyon wind condition.

(3)In the process of leaving the wind field, the average lift and overturning moment of the front car under the constant wind field are larger than that of the canyon wind field, and the maximum instantaneous difference of the overturning moment is as high as 74.99% of the average value of the lower canyon wind.

Acknowledgments

This research was funded by the project "Research on Lift Cooperative Control Technology of High-Speed Train" of CRRC Qingdao Sifang Locomotive and Rolling Stock Co., Ltd.

References

[1] Fujii T, Maeda T, Ishida H, et al. Wind-induced accidents of train/vehicles and their measures in Japan[J]. Quarterly Report of RTRI, 1999, 40(1): 50-55.

[2] Bettle J, Holloway A G L, Venart J E S. A computational study of the aerodynamic forces acting on a tractor-trailer vehicle on a bridge in cross-wind[J]. Journal of Wind Engineering & Industrial Aerodynamics, 2003, 91(5): 573-592.

[3] Lee B E, Soliman B F. An investigation of the forces on three dimensional bluff bodies in rough wall turbulent boundary layers[J]. Journal of Fluids Engineering, 1977, 99(3): 503.

[4] Wei Y.J, Yang H, Hang X.L. Study on Critical Wind Speed for Vehicle Turnover along Qing-Zang Railway [J]. China Safety Science Journal, 2006, 16(6): 4.

[5] Liang X.J , Xiong X.H. Analysis and comparison of lateral aerodynamic performance on four kinds of cars[J]. Journal of Central South University:, Science and Technology 2006, 37(3): 607-612.

[6] Zhai W, Yang J, Li Z, et al. Dynamics of high-speed train in crosswinds based on an air-train-track interaction model[J]. Wind & Structures An International Journal, 2015, 20(2): 143-168.

[7] Jionghao Cheng, Zhenxu Sun, Shengjun Ju, Guowei Yang, Jun Mao & Dilong Guo (2023) Study on mathematical model construction of typical gorge wind field, Engineering Applications of Computational Fluid Mechanics, 17:1, DOI: 10.1080/19942060.2023.2249132